**11th International Symposium on Magnetic Bearings**
**August 26-29, Nara, Japan**

# A Study on Indirect Suspension of Magnetic Target by Actively Controlled Permanent Magnet

**Akihiro YAMAMOTO, Masayuki KIMURA, Takashi HIKIHARA**
Dept. of Electrical Eng., Kyoto Univ., Katsura, Nishikyo, Kyoto 615-8510, Japan
yamamoto@dove.kuee.kyoto-u.ac.jp, kimura@dove.kuee.kyoto-u.ac.jp, hikihara@kuee.kyoto-u.ac.jp

## ABSTRACT

This paper discusses an indirect suspension of magnetic target through an actively controlled permanent magnet. This proposed system consists of an electromagnet, a permanent magnet and a target mainly. The dynamics of levitated bodies are restricted in one dimension, and the target is sufficiently away from the electromagnet. The target is suspended by a proportional-derivative control with respect to the position and the velocity of the permanent magnet. The aim is to model the dynamics of levitated bodies by magnetic charges. The behaviors of levitated bodies near the reference positions are studied numerically and experimentally. As a result, it is shown that the behaviors of levitated bodies near the reference positions can be described by the proposed model.

## I INTRODUCTION

Recently, the controllable manipulation of single atoms or molecules has attracted much attention as a bottom-up nanotechnology. There exists a method for the manipulation of nano-meter or micro-meter sized target like single atoms or molecules by the mechanical interaction between a target and a tip of a cantilever shown in Fig. 1[1, 2, 3]. The possibility of noncontact suspension and manipulation by a tip of an oscillated cantilever was discussed numerically[4]. Here, it is important to prepare an experimental system for establishing dynamics and control methods. However, the preparation of experimental system is difficult because the target is very small. Then, we discuss a macro-suspension system which is analogous to a nano- or micro-suspension system with a cantilever in its dynamics.

A magnetic force can be utilized as an interaction in a macro-suspension system. For the last few decades, the magnetic suspension systems have been studied by many researchers[5, 6], and the possibility of ultra fine motion control in nano meter order was confirmed[7, 8, 9]. A magnetic suspension system for micromanipulation was also discussed[10]. Thereby, we propose an indirect suspension system, which has

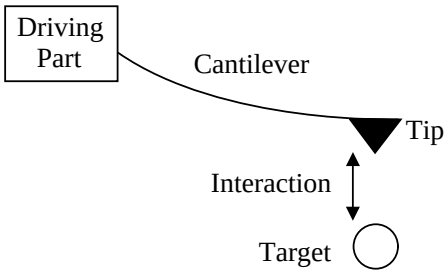


**FIGURE** 1: Schematic diagram of cantilever probe and target.

an analogy with noncontact suspension system with a cantilever. This system consists of an electromagnet, a permanent magnet, and a target, mainly. The dynamics are restricted in one dimension. Moreover, it is assumed that the interaction between the electromagnet and the target is relatively small, when the target is sufficiently away from the electromagnet. This assumption is significant because the target is suspended by the interaction between the target and the actively controlled cantilever probe tip in the nano- or micro-suspension system with a cantilever. Under these settings, the dynamics of indirect suspension system correspond to that of nano- or micro-suspension system with a cantilever. The electromagnet corresponds to the part for driving a cantilever, the permanent magnet to the tip of the cantilever.

The organization of this paper is as follows. In the section Ⅱ, an electromagnet, a permanent magnet, and a target are modeled by magnetic charges. In the section Ⅲ, it is confirmed in a system for suspending a permanent magnet by an electromagnet that the dynamics of levitated body are described by a magnetic charge model. In the section Ⅳ, the equations of motions of levitated bodies and the control method are depicted by a magnetic charge model. The behaviors of levitated bodies are studied numerically and experimentally. As a result, it is confirmed that the behaviors of levitated bodies near

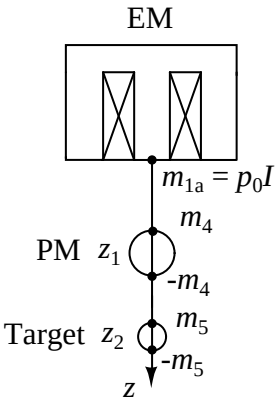


**FIGURE** 2: Magnetic charge model for indirect suspension system.

the reference positions are described by the magnetic charge model. Conclusion is shown in the section V.

## II MAGNETIC CHARGE MODEL

Figure 2 shows the configuration of an electromagnet(EM), a permanent magnet(PM) and a target in an indirect suspension system. The magnetic poles of the EM, the PM and the target are modeled by magnetic charges. For the EM, three magnetic charges are set on the surfaces of the magnetic core respectively because the shape of the magnetic core is E character. However, it is difficult to estimate the each effect of three magnetic charges. Then, a magnetic charge $m_{1a}$ is set on the surface of the magnetic core in $z$-axis as shown in Fig. 2. As the magnetic charge $m_{1a}$ is proportional to the density of the magnetic flux, $m_{1a}$ is proportional to the current $I$ flowing along the EM. Assuming that $m_{1a}$ is also proportional to the current $I$, $m_{1a}$=$p_0 I$. Here, $p_0$ is a proportional coefficient.

For the PM, two magnetic charges $m_4$ and $-m_4$ are set on the surface of the PM as shown in Fig. 2. In this paper, the target is also a permanent magnet. Additionally, the magnetic charges $m_5$ and $-m_5$ are set on the surface of the target.

## III VERIFICATION OF MAGNETIC CHARGE MODEL

In this section, a magnetic charge model is confirmed in a system for suspending a PM by an EM.

### A Equation of Motion and Control Method

In a system for suspending a PM by an EM, the interaction between $m_{1a}$ and $-m_4$ is not considered.

**TABLE** 1: Parameters.

| Physical Quantity | Symbol |
|---|---|
| Acceleration of gravity | $g$ |
| Permeability under vacuum | $\mu_0$ |
| Mass of PM | $M_1$ |
| Mass of target | $M_2$ |
| Radius of PM | $r_1$ |
| Radius of target | $r_2$ |
| Current flowing along EM | $I$ |
| Magnetic point charge for EM | $p_0 I$ |
| Magnetic point charge for PM | $m_4$, $-m_4$ |
| Magnetic point charge for target | $m_5$, $-m_5$ |

The dynamics of the PM are depicted by

$$M_1 \ddot{z}_1 = M_1 g + \frac{m_4 p_0}{4\pi\mu_0} \frac{I}{(z_1 - r_1)^2}, \qquad (1)$$

where the position of $m_{1a}$ is set at the origin, and $z_1$ at the barycentric position of the PM. The parameters of Eq.(1) are given in Table 1 . The first term on the right-hand side is due to the gravity force, and the second to the interaction force between the EM and the PM.

The PM is suspended by proportional-derivative (PD) control with respect to the position and the velocity of the PM. Then, the control output $I$ is set as

$$I = I_0 + I^{\epsilon} = I_0 + K_1(z_1 - \tilde{Z}_{10}) + K_2 \dot{z}_1, \qquad (2)$$

where $I_0$ is the current at an equilibrium state, and the variable with upper suffix $\epsilon$ depicts the deflection from the reference value. Furthermore, $\tilde{Z}_{10}$ is the reference position for the PM in control.

### B Behavior near Reference Position

The PM in the suspension system is a magnetic ball with radius 5 mm. In the numerical simulation, it is absolutely imperative to estimate the proportional coefficient $p_0$ and the magnetic charge $m_4$. For the estimation of $p_0$ and $m_4$, the each magnetic flux distribution generated by the EM and the PM is measured. As results, $p_0$=$3.20 \times 10^{-5}$ Wb/A, $m_4$=$-6.72 \times 10^{-6}$ Wb. By Eq.(1), an equilibrium position $z_{10}$ is derived with respect to the current $I_0$ at an equilibrium state. However, $z_{10}$ is unstable because one of two eigenvalues of the system equation has a positive real part in the system linearized at $z_{10}$. Then, the control gains $K_1$ and $K_2$ are given to stabilize $z_{10}$ by Eqs.(1) and (2). Here, the reference position $\tilde{Z}_{10}$ is determined for $z_{10}$. As an example, the control gains $K_1$=125 A/m, $K_2$=3 As/m are

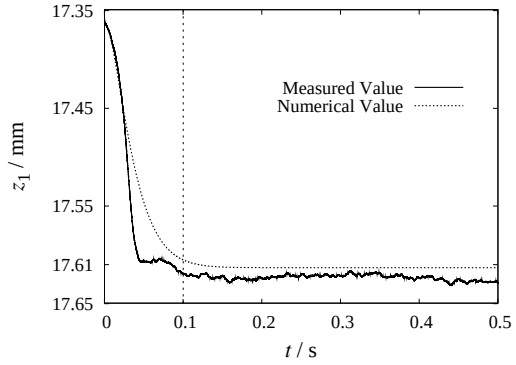


**FIGURE** 3: Behavior of PM.

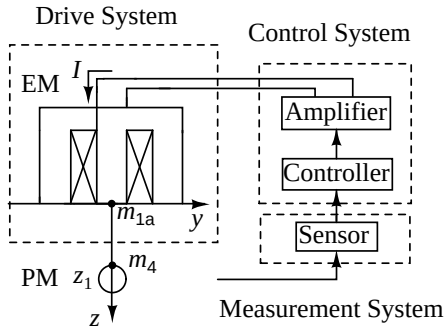


**FIGURE** 4: Schematic diagram of experimental system for suspending PM.

given with respect to the reference values $I_0$=0.30 A, $\tilde{Z}_{10}$=17.61 mm. The behavior of the PM is simulated by Eqs.(1) and (2). The numerical result is shown by the dotted line in Fig. 3.

Figure 4 shows the experimental system for the suspension of PM. The position of the PM is detected by a transmission-type laser position sensor, and the detected position is input to the controller. The control output $I$ amplified appropriately is applied to the EM. As a result, a noncontact suspension of PM is achieved. The experimental result is shown by the solid line in Fig. 3. Here, the reference values and the control gains are same as those in the numerical simulation.

In the range of $t \leq 0.1$ s, the PM moves to the equilibrium position, and is finally suspended at $z_1$=17.62 mm in the experiment. In the numerical simulation, at $z_1$=17.61 mm. The position deflection between the experiment and the numerical simulation is 10 $\mu$m. This is because the detection error of the laser position sensor is $\pm$30 $\mu$m.

In the range of $t > 0.1$ s, the variation is observed in the experiment, and the amount is 10 $\mu$m. On the other hand, the variation is not found in the numerical simulation, because the variation in the experiment is caused by the detection error of the laser position sensor.

The difference between the experimental result and the numerical result is attributed to the detection accuracy of the laser position sensor. Therefore, the numerical result coincides with the experimental result qualitatively. That is, the behavior of the PM near the reference position can be described by Eq.(1).

## C Dependence of Equilibrium Position on Reference Position

The equilibrium positions $Z_{10}$ are derived by Eqs. (1) and (2) as follows:

$$Z_{10} = r_1 - AK_1 \pm \sqrt{(AK_1)^2 - 2A(I_0 - K_1\tilde{Z}_{10} + K_1 r_1)}, \quad (3)$$

where $A$=$(p_0 m_4)/(8\pi\mu_0 M_1 g)$. $Z_{10}^{\rm s}$ and $Z_{10}^{\rm u}$ ($Z_{10}^{\rm s} < Z_{10}^{\rm u}$) denote the equilibrium positions of Eq.(3) respectively. Here, the upper suffix s implies a stable equilibrium position, and the upper suffix u an unstable one. $Z_{10}^{\rm s}$ and $Z_{10}^{\rm u}$ depend on the reference position $\tilde{Z}_{10}$. Then, the position of the PM is detected with respect to the reference position $\tilde{Z}_{10}$ under the settings $I_0$=0.30 A and $K_1$=125 A/m. The experimental result is represented by the symbol '$\times$' in Fig. 5. Moreover, the solid line in Fig. 5 represents the stable equilibrium position $Z_{10}^{\rm s}$ of Eq.(3). As can be seen in Fig. 5, $Z_{10}^{\rm s}$ coincides with the experimental result qualitatively. Therefore, the dependence of equilibrium position on the reference position can be described by Eq.(3) in the range of 16 mm $\leq \tilde{Z}_{10} \leq$ 19 mm. The possibility is confirmed at another control gain.

## D Dependence of Equilibrium Position on Control Gain

$Z_{10}^{\rm s}$ and $Z_{10}^{\rm u}$ depend on the control gain $K_1$ as can be seen in Eq.(3). Then, the position of the PM is detected with respect to the control gain $K_1$ under the settings $I_0$=0.30 A and $\tilde{Z}_{10}$=17.35 mm. The experimental result is represented by the symbol '$\times$' in Fig. 6. $Z_{10}^{\rm s}$ and $Z_{10}^{\rm u}$ are respectively shown by the solid line and the dotted line in Fig. 6. In the experiment, the PM is able to be suspended at any control gain $K_1$ in the range of 33 A/m $\leq K_1 \leq$ 150 A/m. Moreover, the PM moves toward the EM as $K_1$ becomes small. The change in the range of $K_1 \geq$ 60 A/m is much smaller than that in the range of $K_1 <$ 60 A/m. The stable equilibrium position $Z_{10}^{\rm s}$ shown in Fig. 6 represents the characteristics similar to the experiment.

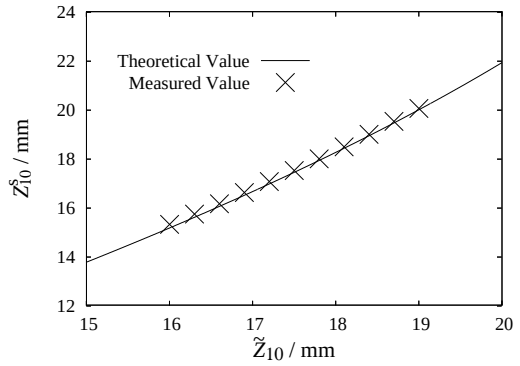


**FIGURE** 5: Equilibrium position $Z^{s}_{10}$ with respect to $\tilde{Z}_{10}$ at $K_1$=125 A/m.

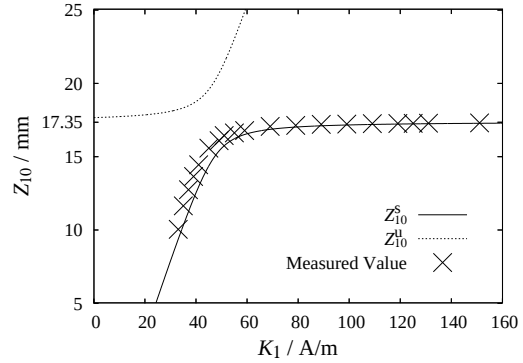


**FIGURE** 6: Equilibrium positions $Z^{s}_{10}$ and $Z^{u}_{10}$ with respect to $K_1$ at $\tilde{Z}_{10}$=17.35 mm.

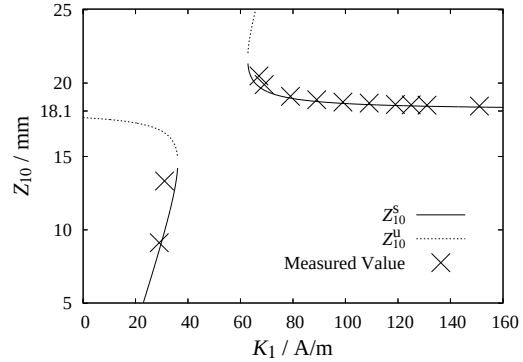


**FIGURE** 7: Equilibrium positions $Z^{s}_{10}$ and $Z^{u}_{10}$ with respect to $K_1$ at $\tilde{Z}_{10}$=18.1 mm.

Additionally, the position of the PM is detected under the settings $I_0$=0.30 A and $\tilde{Z}_{10}$=18.1 mm. The symbol '×' in Fig. 7 shows the experimental result. The solid line and the dotted line show $Z^{s}_{10}$ and $Z^{u}_{10}$. In the experiment, the PM is not able to be suspended with respect to any control gain $K_1$ in the range of 31 A/m $< K_1 <$ 67 A/m. In the range of $K_1 \geq$ 67 A/m, the PM gets away from the EM as $K_1$ becomes small. On the other hand, the PM approaches the EM in the range of $K_1 \leq$ 31 A/m. $Z^{s}_{10}$ in Fig. 7 also represents the characteristics similar to the experiment. Therefore, the theoretical results obtained by Eq.(3) coincide with the experimental results qualitatively. That is, the dependence of equilibrium position on the control gain $K_1$ can be described by Eq.(3) in the range of 30 A/m $\leq K_1 \leq$ 150 A/m.

# IV INDIRECT SUSPENSION OF MAGNETIC TARGET

## A Equations of Motions

In the indirect suspension system, the interaction between $m_{1a}$ and $-m_4$ is not considered. So is the interaction between $m_{1a}$ and $-m_5$. The dynamics of levitated bodies are depicted by

$$\begin{cases} M_1\ddot{z}_1 = M_1 g + F_1 - f_1 - f_2 - f_3 - f_4, \\ M_2\ddot{z}_2 = M_2 g + F_2 + f_1 + f_2 + f_3 + f_4, \end{cases} \tag{4}$$

$$\begin{cases} F_1 = \dfrac{m_4 p_0}{4\pi\mu_0}\dfrac{I}{(z_1 - r_1)^2}, \\ F_2 = \dfrac{m_5 p_0}{4\pi\mu_0}\dfrac{I}{(z_2 - r_2)^2}, \\ f_1 = \dfrac{m_4 m_5}{4\pi\mu_0}\dfrac{1}{(z_2 - r_2 - z_1 + r_1)^2}, \\ f_2 = -\dfrac{m_4 m_5}{4\pi\mu_0}\dfrac{1}{(z_2 + r_2 - z_1 + r_1)^2}, \\ f_3 = -\dfrac{m_4 m_5}{4\pi\mu_0}\dfrac{1}{(z_2 - r_2 - z_1 - r_1)^2}, \\ f_4 = \dfrac{m_4 m_5}{4\pi\mu_0}\dfrac{1}{(z_2 + r_2 - z_1 - r_1)^2}, \end{cases} \tag{5}$$

where the position of $m_{1a}$ is set at the origin, $z_1$ and $z_2$ at the barycentric positions of the PM and the target, respectively. The parameters of Eqs.(4) and (5) are given in Table 1 . Moreover, $F_1$ denotes the interaction between the EM and the PM, and $F_2$ between the EM and the target. $f_i$ ($i$=1, 2, 3, 4) denotes an interaction between the PM and the target.

## B Control Method

In the indirect suspension system, the target is sufficiently away from the EM. The target is suspended only by the PM because the interaction between the EM and the target can be neglected. As the magnetic force of the PM is constant, the distance between the PM and the target is kept constant at an equilibrium state. Therefore, the target can be suspended by changing the reference position for the

**TABLE** 2: Reference values.

| | $I_0$ /A | $\tilde{Z}_{10}$ /mm | $\tilde{Z}_{20}$ /mm |
|---|---|---|---|
| $\alpha$ | 0.40 | 17.41 | 35.89 |
| $\beta$ | 0.40 | 17.41 | 36.37 |
| $\gamma$ | 0.40 | 17.44 | 35.80 |

**TABLE** 3: Control gains.

| | $K_1$/A/m | $K_2$/A/m | $K_3$/As/m | $K_4$/As/m |
|---|---|---|---|---|
| $\alpha$ | 70.0 | 6.50 | 0.13 | -2.5 |
| $\beta$ | 48.2 | 4.83 | 0.13 | -2.2 |
| $\gamma$ | 53.0 | 5.30 | 0.13 | -3.3 |

PM in control according to the change of the distance between the PM and the target. The control output $I$ is set as

$$\begin{cases} I = I_0 + I^{\epsilon}, \\ \quad = I_0 + K_1(z_1^{\epsilon} - z^*) + K_4 \dot{z}_1, \\ z^* = K_2(z_2^{\epsilon} - z_1^{\epsilon}) + K_3(\dot{z}_2 - \dot{z}_1), \end{cases} \tag{6}$$

where the variables with upper suffix $\epsilon$ depict the deflections from the reference values respectively. Moreover, $z^*$ is the controlled value with respect to the distance between the PM and the target. $\tilde{Z}_{10}$ and $\tilde{Z}_{20}$ are the reference positions for the PM and the target in the control.

## C Numerical Simulation

The PM in the indirect suspension system is a magnetic ball with radius 5 mm, and the target is one with radius 4 mm. In the numerical simulation, it is absolutely imperative to estimate the magnetic charge $m_5$. The magnetic flux distribution generated by the target is measured for the estimation. As a result, $m_5$=$-3.47 \times 10^{-6}$ Wb. By Eqs.(4) and (5), the each equilibrium position $z_{10}$ and $z_{20}$ is derived with respect to the current $I_0$ at an equilibrium state. However, $z_{10}$ and $z_{20}$ are unstable because two of four eigenvalues of the system equation have the positive real parts in the indirect suspension system linearized at $z_{10}$ and $z_{20}$. Then, the control gains $K_1$, $K_2$, $K_3$ and $K_4$ are given to stabilize $z_{10}$ and $z_{20}$. Here, $\tilde{Z}_{10}$ and $\tilde{Z}_{20}$ are determined for $z_{10}$ and $z_{20}$. The dotted lines in Figs. 8 and 9 represent the behaviors of levitated bodies and the control output $I$, respectively. The reference values and the control gains in the numerical simulation are shown by $\alpha$ in Tables 2 and 3. Moreover, the control output $I$ is applied to the EM at 0 s. As can be seen in Figs. 8 and 9, the PM approaches the target first, and then the target is levitated. Finally, the PM is suspended at the reference position for the PM in control, and the target at the reference position for the target. The control output $I$ converges to the reference current $I_0$.

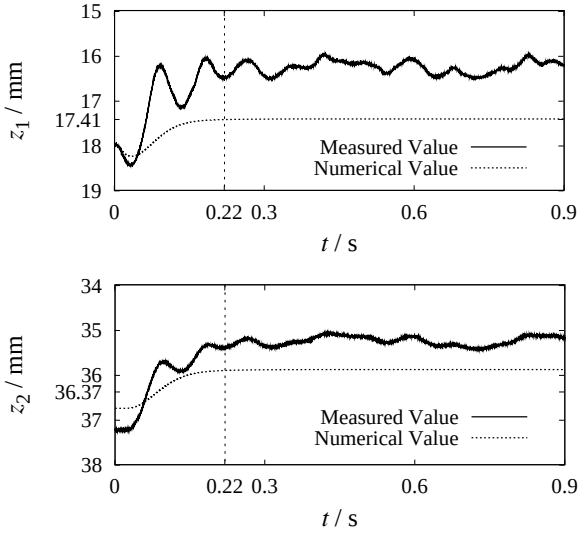


**FIGURE** 8: Behaviors of levitated bodies.

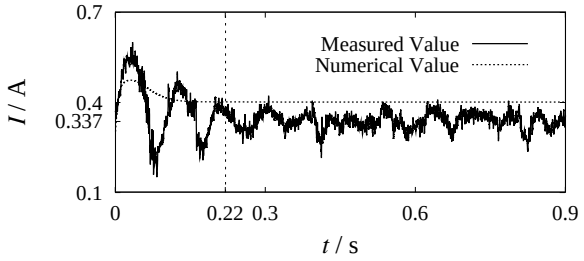


**FIGURE** 9: Control output $I$.

By these results, it is confirmed numerically that the target is suspended at the reference position for the target through the actively controlled PM.

## D Experiment

Figures 10 and 11 show the indirect suspension system and a diagram of a controller, respectively. In this experimental system, the positions of levitated bodies are detected by transmission-type laser position sensors. The detected positions are utilized as the inputs of the controller. The control output $I$ amplified appropriately is applied to the EM, and the PM is controlled actively by the EM. As a result, the indirect suspension of target is achieved through the actively controlled PM. The photograph of the achieved indirect suspension is shown in Fig. 12.

The experimental results are represented by the solid lines in Figs. 8 and 9. Here, the reference values and the control gains are shown by $\beta$ of Tables 2 and

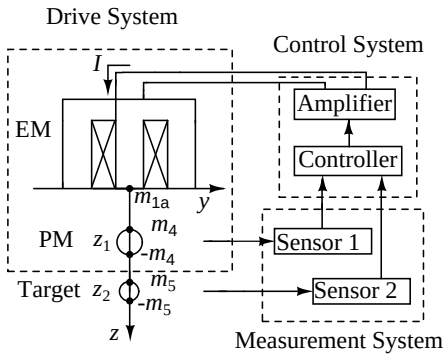


**FIGURE** 10: Schematic diagram of experimental system for suspending target indirectly through actively controlled PM.

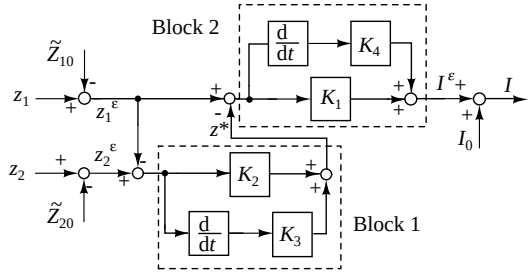


**FIGURE** 11: Block diagram of controller.

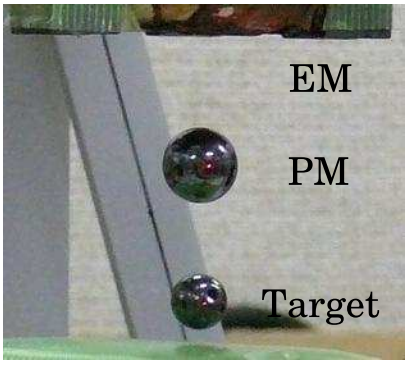


**FIGURE** 12: Indirect suspension of magnetic target through actively controlled PM.

3. In the range of $t \leq 0.22$ s, the target moves toward the EM every time the PM approaches the target. At $t$=0.22 s, the PM is levitated at $z_1$=16.50 mm, and the target is suspended at $z_2$=35.40 mm. Then, the deflection between the position of the PM and the reference position is 0.91 mm, and the deflection is 0.97 mm for the target. Moreover, the control output $I$ is 0.337 A. These deflections are caused by the difference between the reference positions of levitated bodies and the equilibrium positions of experimental system with respect to the current $I_0$ at the equilibrium state.

In the range of $t > 0.22$ s, each of levitated bodies moves up and down near the position at $t$=0.22 s. The both amplitudes are 0.5 mm. Additionally, the control output $I$ changes near 0.337 A, and the amount of change is 0.1 A. In the experiment, the positions of levitated bodies are detected on $z$-axis by laser position sensors. The each displacement of levitated bodies in the $y$-axis direction is detected as the displacement in the $z$-axis direction, because the shape of the PM and the target is ball. The motions of levitated bodies and the change of control output $I$ are observed as this detected positions are input to the controller.

## E Evaluation of Equations of Motions

In the experiment, it is difficult to determine the reference positions for the equilibrium positions of the experimental system with respect to $I_0$ because of the estimation errors of $p_0$, $m_4$ and $m_5$. Then, we focus attention on the change of the control output $I$. The reference values and the control gains are calculated for getting the similar result to the experimental result. $\gamma$ in Tables 2 and 3 show the calculated values. Figs. 13 and 14 represent the behaviors of levitated bodies near the reference positions and the control output $I$, respectively. From Fig. 14, it is verified that the numerical result is qualitatively similar to the experimental result. Here, the reference values and the control gains in the numerical simulation are different from those in the experiment. This difference is caused by the estimation errors of $p_0$, $m_4$ and $m_5$.

In the range of $t \leq 0.22$ s, the PM and the target are oscillated and levitated. Near the each reference position, the amplitude and the cycle of the oscillation coincide with those in the experiment qualitatively.

In the range of $t > 0.22$ s, the oscillations of levitated bodies become small, and finally the PM is suspended at the position from the reference position $z_1^\epsilon$=−1.07 mm, and the target at $z_2^\epsilon$=−1.08 mm. The deflection changes of levitated bodies are different from those in the experiment. Additionally, the convergence of the change is also different. These difference arise because the motions of levitated bodies in the $y$-axis direction are not considered in the numerical simulation.

Therefore, the numerical results coincide with the experimental results qualitatively. That is, the dynamics of levitated bodies near the reference positions can be described by Eqs.(4) and (5).

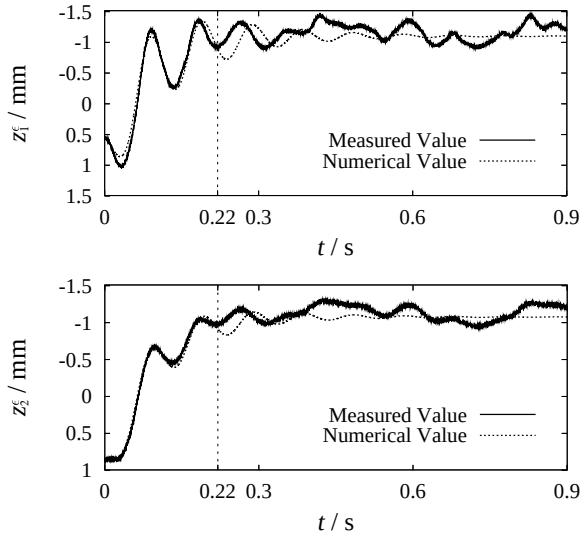


**FIGURE** 13: Deflection changes of levitated bodies from reference positions.

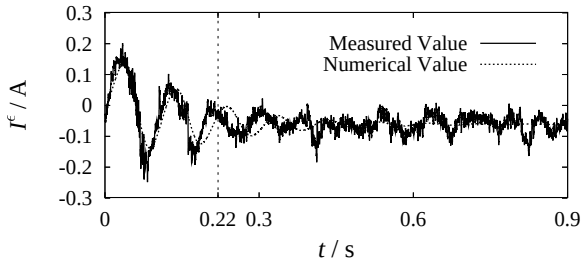


**FIGURE** 14: Deflection change of control output $I$ from reference current $I_0$.

## V CONCLUSION

In this paper, an indirect suspension of magnetic target through an actively controlled PM is discussed. The EM, the PM and the target are described by magnetic charges. It was confirmed that the dynamics of the PM were described by a magnetic charge model in a system for suspending a PM.

A magnetic charge model is applied to an indirect suspension system, and the equations of motions of levitated bodies are depicted. The control method is also set. Here, the target is suspended by PD control with respect to the position and the velocity of the PM. Then, the possibility of indirect suspension was confirmed numerically and experimentally. Additionally, it was confirmed that the behaviors of levitated bodies near the reference positions were described by the depicted equations of motions of levitated bodies.

In addition, the dependences of equilibrium positions on the reference values and the control gains should be studied experimentally and numerically. The obtained results will be important to establish the dynamics and the control methods of the nano- or micro-suspension systems with a cantilever.

## REFERENCES

(1) Y. Sugawara, Y. Sano, N. Suehira, and S. Morita, Atom manipulation and image artifact on Si(1 1 1)7×7 surface using a low temperature noncontact atomic force microscope, Appl. Surf. Sci., Vol.188, 285-291, 2002.

(2) N. Oyabu, O. Custance, I. Yi, Y. Sugawara, and S.Morita, Mechanical Vertical Manipulation of Selected Single Atoms by Soft Nanoindentation Using Near Contact Atomic Force Microscopy, Phys. Rev. Lett. Vol.90, No.17, 2003.

(3) B. Kim, T. Hikihara, and V. Putkaradze, Numerical Study of Atom Interchange on Material Surface under Periodic Force, Proc. NOLTA'07, Canada, 184-187, 2007.

(4) T. Hikihara, and K. Yamasue, A Numerical Study on Suspension of Molecules by Microcantilever Probe, Proc. LDIA2005 *Kobe − Awaji*, JAPAN, 29-32, 2005.

(5) E. Shameli, M. B. Khamesee. and J. P. Huissoon, Nonlinear controller design for a magnetic levitation device, Microsyst. Technol., Vol.13, No.8-10, 831-835, 2007.

(6) H. Bleuler, A Survey of Magnetic Levitation and Magnetic Bearing Types, JSME Int. J., Ser. Ⅲ, Vol.35, No.3, 335-342, 1992.

(7) Z. Zhang, and C–H. Menq, Six–Axis Magnetic Levitation and Motion Control, IEEE Trans. Robotics, Vol.23, No.2, 196-205, 2007.

(8) M. Golob, and B. Tovornik, Modeling and control of the magnetic suspension system, ISA Trans., Vol.42, 89-100, 2003.

(9) S–K. Kuo, X. Shan, and C–H. Menq, Large Travel Ultra Precision $x$–$y$–$\theta$ Motion Control of a Magnetic–Suspension Stage, IEEE/ASME Trans. on Mechatronics, Vol.8, No.3, Sept., 334-341, 2003.

(10) D. Craig, and M. B. Khamesee, Motion control of a large gap magnetic suspension system for microrobotic manipulation, J. Phys. D: Appl. Phys., Vol.40, 3277-3285, 2007.